

Matched filter analysis of burst waveform injections

M. Sung for the LSC

Louisiana State University, Baton Rouge, LA, 70803 USA

E-mail: sung@phys.lsu.edu

Abstract. Hardware injections provide us with a crucial tool for proving that we understand the response and performance of the LIGO detectors. Since we have complete knowledge of the injected waveform and detailed measurements of the detector response function, we are able to predict and confirm the instrument response. During the S5 science run of LIGO, various burst-type waveforms are being injected. We have analyzed the first seven months of these injections, using optimal matched filters derived from the injection waveforms. We have confirmed that most of the responses follow the predictions and have measured the accuracy of the estimated arrival time. In addition, we examined transients identified by the *KleineWelle* algorithm in auxiliary data channels at the time of hardware injections. Through this study, we could recognize couplings between auxiliary channels and the gravitational wave channels and assess the safety of the use of auxiliary channels as vetoes for gravitation wave candidates.

LIGO-P070036-01-Z

PACS numbers: 04.80.Nn, 95.55.Br, 95.75.-z

1. Introduction

The LIGO observatories are currently collecting the data for their first long observing run at design sensitivity; this run began in November of 2005, and is designated as ‘‘S5’’. During this run, hardware injections with various waveforms have been carried out to monitor the response and performance of the detectors. Hardware injections provide the only direct test of the entire system.

In this article, we describe how hardware injections are performed, and the techniques used to analyze the injection data. The primary analysis tools are linear filters: whitening filters, and filters matched to the injected waveforms. These methods were applied to recover the strength and timing of each injection, and compare them with expectations. This study shows that we have a good quantitative understanding of the total system response.

In addition, we used a transient search technique called the KleineWelle algorithm [1], to check the response of auxiliary channels to hardware injections, which shows how the coupling between those channels and strain sensing channels can be tested.

2. Hardware injection procedures

Burst-type hardware injections are performed with twenty distinct waveforms, as listed in Table 1. Usually a subset of these are used in a single injection period, and the magnitude and time offsets are varied in a systematic fashion. The same waveforms are injected into all three interferometers at the same time with small (a few ms) or no time shifts between the detectors. These planned injection periods take place several times each day at irregular intervals.

The crucial parts of the interferometer are shown in Fig. 1 as a highly simplified block diagram of the ‘‘differential-arm’’ servo system. The total strain measured by the antenna (noise plus gravitational wave) is shown as the quantity $s(t) = n(t) + h(t)$. The observable output of the system is the error signal $e(t)$, recorded from the channel called DARM_ERR. The many components of the system can be condensed into three linear response functions, specified in the frequency domain: a ‘‘Sensing’’ function $C(f)$, a ‘‘Digital Filter’’ function $D(f)$, and an ‘‘Actuation’’ function $A(f)$. The actuation function is further divided into functions for each arm $A_x(f)$ and $A_y(f)$ and coupling coefficients k_x, k_y ,

$$A(f) = k_x A_x(f) - k_y A_y(f). \quad (1)$$

Then the servo system can be solved to find the response function of the detector $R(f)$, which converts the error signal $e(f)$ into the strain signal $s(f)$,

$$s(f) = \frac{1 + C(f)D(f)A(f)}{C(f)} e(f) \equiv R(f)e(f), \quad (2)$$

where $e(f)$, $s(f)$ are the Fourier transforms of $e(t)$, $s(t)$.

Injections are done by adding prepared waveforms to the excitation channel on the x -arm, ETMX_EXC. The waveforms for injection, $a_x(t)$, are prepared by applying the

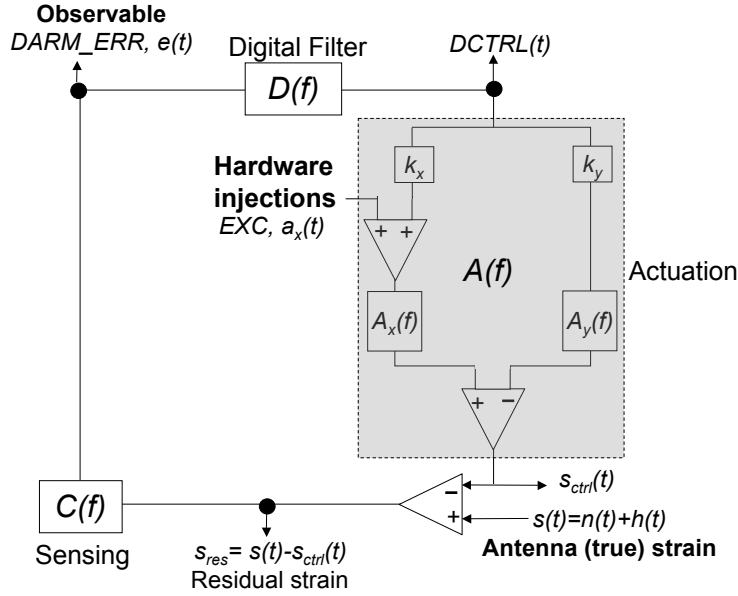


Figure 1. A simplified block diagram of the differential arm servo system of the LIGO detector. The optics and analog electronics are represented in the Sensing block, the digital electronics in the Digital Filter block, and the mechanical components in the Actuation block. Their transfer functions are specified by frequency domain functions, such as $C(f)$.

actuation function, $A_x(f)$, in the frequency domain, to waveforms generated in strain, $h_{inj}(t)$,

$$a_x(f) = -\frac{h_{inj}(f)}{A_x(f)}, \quad (3)$$

and then transforming back into the time domain. The time series of this waveform is then injected into the differential arm servo. A sample injection of a Gaussian with a short width of 0.3 ms, carried out at $t_{gps} = 833364049$, is shown in Fig. 2. The waveform injected to the excitation channel is shown in Fig. 2 a) and the desired waveform in strain, $h_{inj}(t)$, is shown in Fig. 2 b). The designed time offset (0.5 s) from the injection time and magnitude ($20 \times 10^{-21} \sqrt{s}$) scaling for this specific injection are applied. The detector response to this injection measured in the error signal channel DARM_ERR, $e(t)$, is shown in Fig. 2 c) and d) with two different time scales.

3. Linear filters

Two different whitening filters are applied to the data to examine the error signal response $e(t)$ to each injection with the noise reduced.

$$e_{sw}(t') = \int_{-\infty}^{\infty} df e^{-i2\pi ft'} \frac{1}{\sqrt{S_n(f)}} e(f), \quad (4)$$

for single whitening and

$$e_{dw}(t') = \int_{-\infty}^{\infty} df e^{-i2\pi ft'} \frac{1}{S_n(f)} e(f), \quad (5)$$

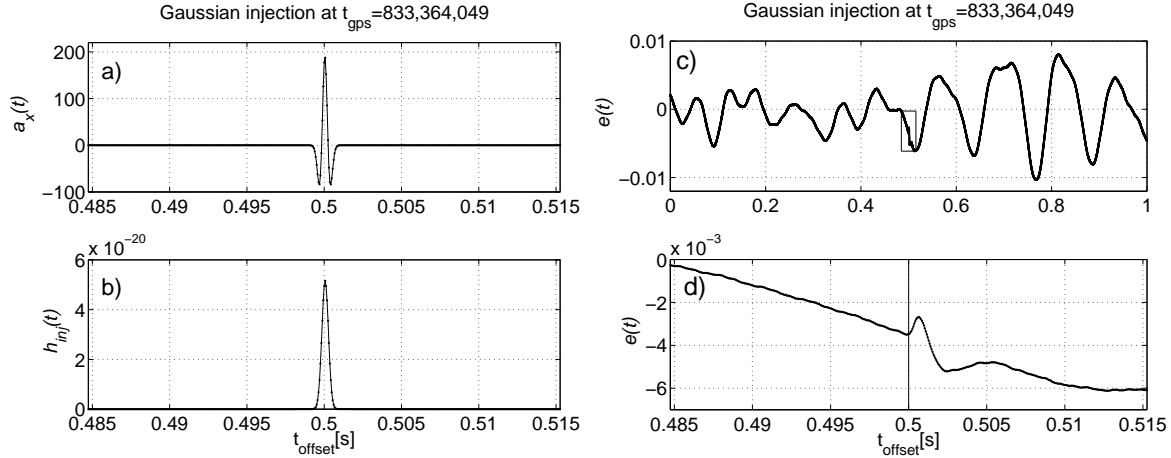


Figure 2. Hardware injection with a Gaussian impulse with $\tau = 0.3$ ms done at $t_{\text{gps}} = 833,364,049$: waveforms a) injected to ETMX_EXC and b) desired in strain as $h_{\text{inj}}(t)$, and c) error signal data $e(t)$ at the injection time and d) the same data with finer time scale.

for double whitening, where $S_n(f)$ is the power spectral density of the noise, estimated from the data.

The primary analysis used is the optimal linear filter [2], a standard method from classical signal processing for known signal waveforms. The optimal filter is the matched filter optimized with the double whitening filter:

$$\|h_\alpha(t')\| = N_\alpha \int_{-\infty}^{\infty} df e^{-2\pi i f t'} \tilde{h}_\alpha^*(f) \frac{1}{S_n(f)} s(f). \quad (6)$$

Here $\|h_\alpha(t')\|$ is the output time series from the optimal filter with the template, $h_\alpha(t)$, and $s(f)$ and $\tilde{h}_\alpha(f)$ are the Fourier transforms of the strain data, $s(t)$, and $h_\alpha(t)$, respectively. The normalization factor, N_α , in eq. (6), is derived to have the unbiased strength measurement of the reconstructed signal waveform as the maximum of the filtered output, calculated in units of the norm of waveform, $\|h_\alpha\| \equiv \sqrt{\int h_\alpha^*(t) h_\alpha(t) dt}$. The injected waveform, $h_{\text{inj}}(t)$ in Eq. (3), is used as the template waveform $h_\alpha(t)$.

By using relations (2) to convert the template waveform, h_α , and the noise spectrum, S_n in strain into functions of the error signal, $e(t)$ and S_m , it can be seen that the equivalent formula for the optimal filter can be written for the error signal data, after the effect of the response function is cancelled out:

$$\|h_\alpha(t')\| = N_\alpha \int_{-\infty}^{\infty} df e^{-2\pi i f t'} \tilde{k}_\alpha^*(f) \frac{1}{S_m(f)} e(f), \quad (7)$$

where k_α and S_m are the template waveform and the noise spectrum in terms of the error signal. This implies the optimal filter can be applied to either the strain data, $h(t)$, or the error signal data, $e(t)$, to get the same filtered output, $\|h_\alpha(t')\|$.

To use the discrete fourier transform, the data were segmented as shown in Fig. 3. An injection period starts 5 s before the first injection and ends 5 s (or more) after the last injection. The injection period is divided into 64 s segments with 16 s overlapping

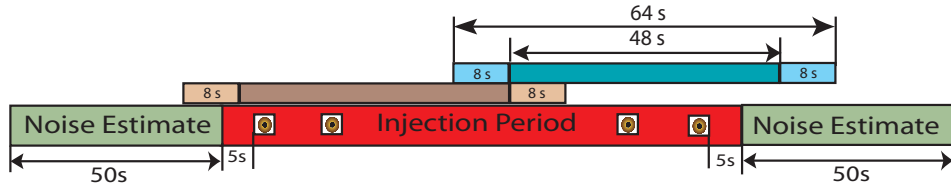


Figure 3. Time segmentation of the analysis. The injection period with injections is divided into 64 s segments with 16 s overlapping with the next segment. Noise spectrum is obtained from data of 50 s before and after the injection period.

with the next segment. The raw data from each analysis segment of 64 s is multiplied by a Tukey window [3] (flat over the middle 62 s), then Fourier transformed, then filtered, and finally transformed back to the time-domain. The first segment starts 10 s before the first injection. After testing with various waveforms and different setups, to avoid discontinuity at the boundary of each segment, the middle 48 s of each time segment is kept, and the 8 s at each end are discarded. The power spectral density of the noise (for constructing the whitening and optimal filters) was calculated from two 50 s long data before and after the injection period. Template waveforms, $h_\alpha(t)$, are obtained by reading the text files of strain waveforms injected, and elongated to 64 s long by padding with zeros.

4. Results

Figure 4 shows the single (a) and double (b) whitened error signal data with an injection of the Gaussian impulse shown in Fig. 2, as well as the expected curve for the injected Gaussian waveform with the same whitening filter and with the proper scaling and offset in time. Both whitened spectra agree well with the expected curves.

The filtered output of this same injection obtained from the optimal filter with the template of the injected Gaussian waveform is shown in Fig. 4 c) and d) in two different time scales. Figure 4 d) demonstrates how the strength and timing of injection are measured. The measured strength ($\|h_{\text{GA03}}\| = 19.984 \times 10^{-21} \sqrt{\text{s}}$) and timing ($t_{\text{offset}} = 0.5001 \text{ s}$) of this injection agree with the injected values to within a few percent. The root-mean-squared (RMS) noise level around this injection period after filtering is $\sigma_{\text{noise}} = 0.0357 \times 10^{-21} \sqrt{\text{s}}$, which is larger than the difference between the injected and measured strengths.

A more realistic example from an injection of a supernova waveform, the Zwerger-Müller $A3B3G1$ [4], is shown in Fig. 5. The injection was done with $\|h_{\text{ZM}}\| = 0.6 \times 10^{-21} \sqrt{\text{s}}$ and $t_{\text{offset}}^{\text{injected}} = 0.3555 \text{ s}$, and was recovered with $\|h_{\text{ZM}}\| = 0.6661 \times 10^{-21} \sqrt{\text{s}}$ ($\sigma_{\text{noise}} = 0.0417 \times 10^{-21} \sqrt{\text{s}}$) and $t_{\text{offset}}^{\text{measured}} = 0.3558 \text{ s}$. It is noticeable in this example that the time measurement is the offset time, rather than the peak time of the waveform. This is the result expected from using the matched filter.

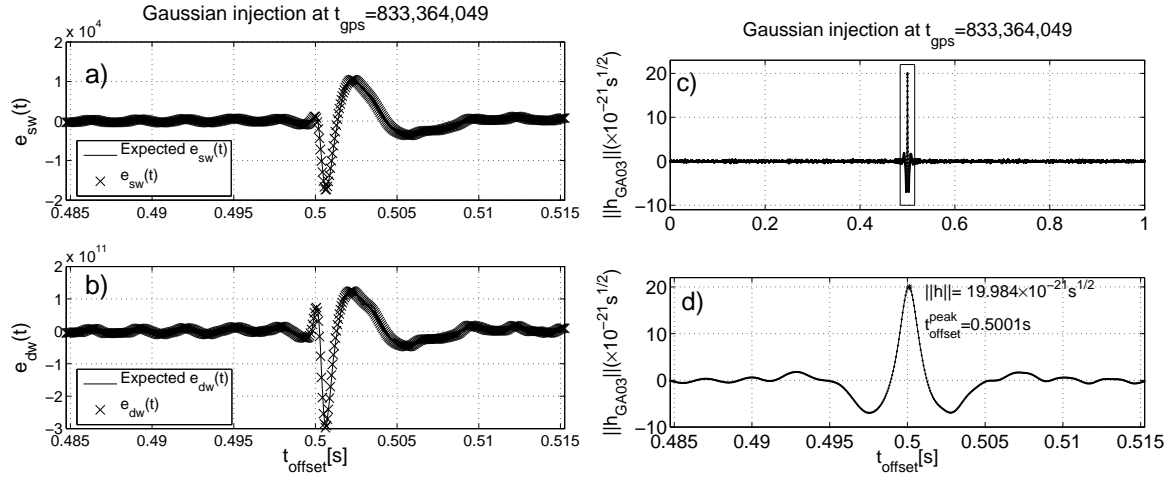


Figure 4. Output time series for an injection of the Gaussian pulse of Fig. 2 from a) single and b) double whitening filters and the optimal linear filter with two different time scales in c) and d). Measurement of strength and offset time are demonstrated in d).

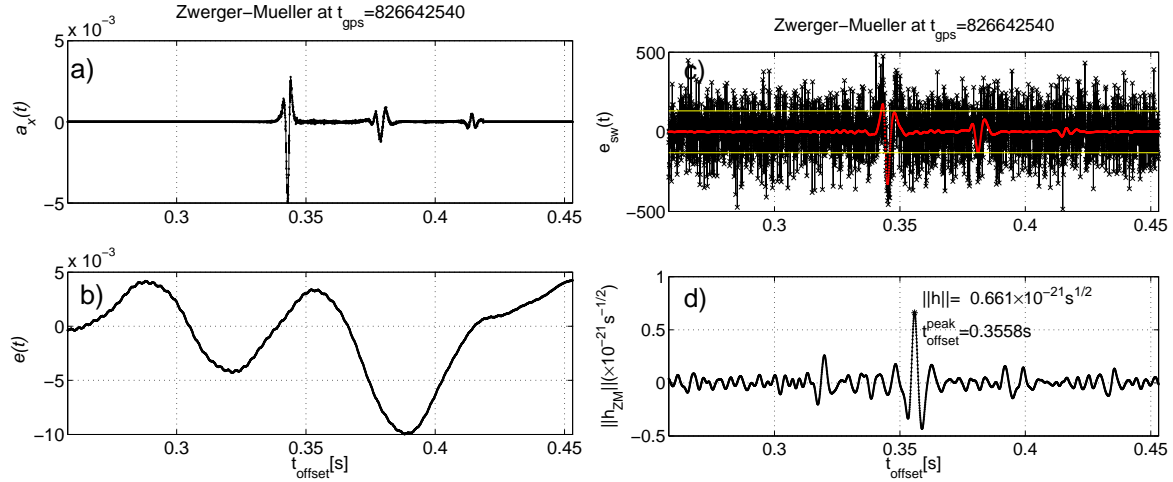


Figure 5. Injection of Zwerger-Mueller ($A3B3G1$) waveforms: a) waveform injected in ETMX_EXC, b) error signal data recorded at the channel DARM_ERR, filtered outputs from c) single whitening filter (with the expected signal waveform from the injection) and d) the optimal filter. Measurement of strength and time offset is shown in d).

5. Statistical analysis

This report used hardware injections over about 7 months from January 20, 2006 to August 28, 2006, from all three interferometers in LIGO - the 4 km detector (L1) at the Livingston observatory and the 4 km (H1) and 2 km (H2) detectors at the Hanford observatory. During this period, a total of 4098 burst injections were carried out in L1 and 5018 and 5958 injections were done in H1 and H2 respectively. Table 1 shows how many injections were made for each of the 20 burst waveforms at each detector. Eight waveforms, including a Gaussian with $\tau = 1$ ms or sine-Gaussian with 70 Hz ($Q = 9$),

Table 1. Numbers of hardware injections on each detector.

Injected waveform	L1	H1	H1
Gaussian $\tau = 0.3$ ms	40	48	52
Gaussian $\tau = 1$ ms	478	581	677
Gaussian $\tau = 3$ ms	40	48	52
Gaussian $\tau = 10$ ms	40	48	52
sine-Gaussian 50 Hz, $Q = 9$	34	46	58
sine-Gaussian 70 Hz, $Q = 9$	474	578	692
sine-Gaussian 100 Hz, $Q = 9$	34	46	58
sine-Gaussian 153 Hz, $Q = 9$	34	46	58
sine-Gaussian 235 Hz, $Q = 9$	472	579	683
sine-Gaussian 393 Hz, $Q = 9$	34	46	58
sine-Gaussian 554 Hz, $Q = 9$	34	46	58
sine-Gaussian 850 Hz, $Q = 9$	34	46	58
sine-Gaussian 914 Hz, $Q = 9$	440	524	634
sine-Gaussian 1304 Hz, $Q = 9$	34	46	58
sine-Gaussian 2000 Hz, $Q = 9$	472	579	683
sine-Gaussian 3068 Hz, $Q = 9$	34	46	58
Zwenger-Müller (A3B3G1)	430	527	617
Cosmic string cusp $f_{\text{cutoff}} = 220\text{Hz}$	430	527	617
Band-limit white noise, 250 Hz, $\delta f = 100$ Hz, $\sigma = 30\text{ms}$	440	524	634
Ringdown 2600 Hz, $\delta t = 30$ ms	70	95	101
Total	4098	5018	5958

were injected more often and with more variety of strengths than others.

Each waveform was analyzed in terms of the measured strength and time offset. An example, a Gaussian with width $\tau = 1$ ms, is shown in Fig. 6. The gps time dependence of measurements in Fig. 6 a) and d) shows that the performance of the detector can be monitored over time by recovering signals from hardware injections. Measured strengths are compared with the injected strengths in Fig. 6 b). The difference between injected and measured time offsets of injections is shown as a function of the injected strengths in Fig. 6 e). Uncertainties in strength and time measurements with this waveform can be estimated with a Gaussian fit as shown in Fig. 6 c) and f). It is noticeable that injections with lower strengths have more uncertainty in both strength and time. The discreteness of the time measurement histogram in Fig. 6 is caused by a discrete estimate of the arrival time.

Figure 7 shows how the eight waveforms from Table 1 injected the most time are measured by all three detectors. Fluctuations in the strength measurement are comparable with the noise level around the injections, and the time measurement is in agreement within a few ms with the injection time for all three detectors.

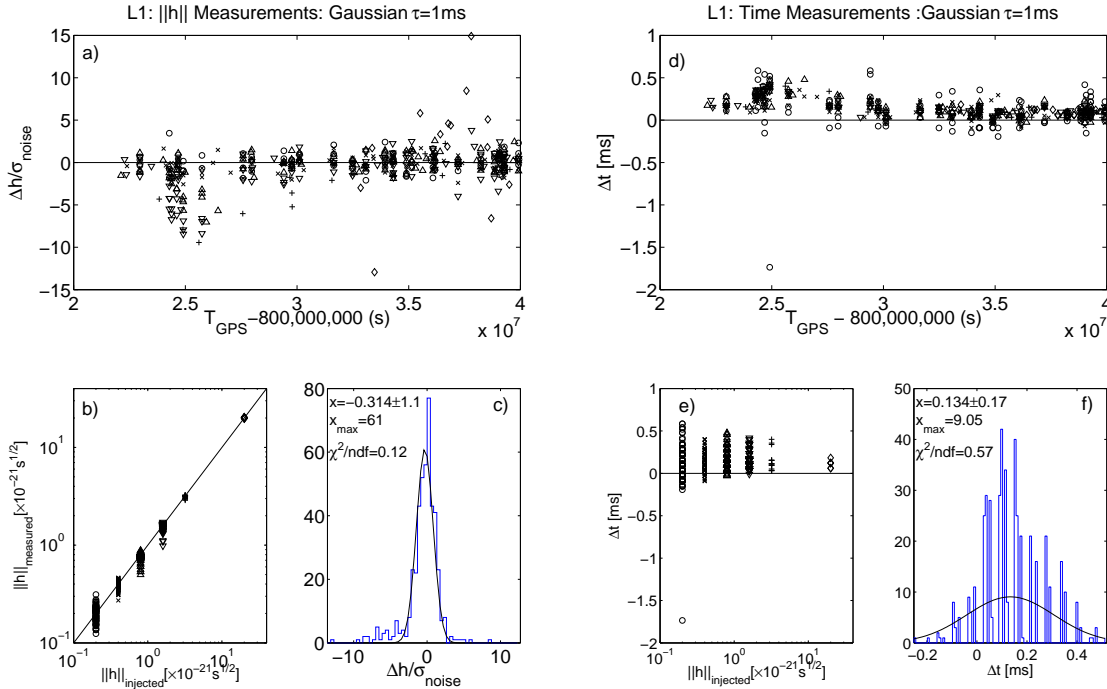


Figure 6. Measurement of strengths and time of injections with a Gaussian with the width of $\tau = 1$ ms at L1: a) gps time dependence of differences in the strength measurements ($\Delta h \equiv ||h||_{\text{measured}} - ||h||_{\text{injected}}$) in term of noise level (σ_{noise}), b) injected strengths vs. measured strengths of injections, c) distribution of differences of $\Delta h/\sigma_{\text{noise}}$, d) gps time dependence of differences of time measurements ($\Delta t \equiv t_{\text{offset}}^{\text{measured}} - t_{\text{offset}}^{\text{injected}}$), e) Δt vs. $||h||_{\text{injected}}$, and f) Δt distribution. The mean and standard deviation of the distribution of Δh is $(0.31 \pm 1.1) * \sigma_{\text{noise}}$, and for Δt , it is (0.13 ± 0.17) ms. The same symbol assignment is used in a), b), d) and e), to show different injected strengths.

6. Coupling between auxiliary channels and gravitational wave channels

In the LIGO experiment many auxiliary channels are recorded as data to monitor the performance of detector and environmental changes during the experiment. These channels are not designed to detect any real signal from gravitational wave sources, so any signal candidates with excess strength in these channels can not be good candidates for a gravitational wave. In other words, these auxiliary channels can be very useful to veto some events as gravitational wave candidates. However, for various reasons, it is possible that some of these channels are influenced by a signal from a real gravitational wave source if there is a coupling with the gravitational wave channel.

Hardware injections, which simulate realistic signal events in the detector, provide a useful tool to test whether an auxiliary channel has any coupling to the gravitational wave channel. The KleineWelle algorithm, which was developed to search for transients, was applied to many auxiliary channels at the time of injections. For this study, injections of 272 days from the S5 run were used. Many of these channels are found

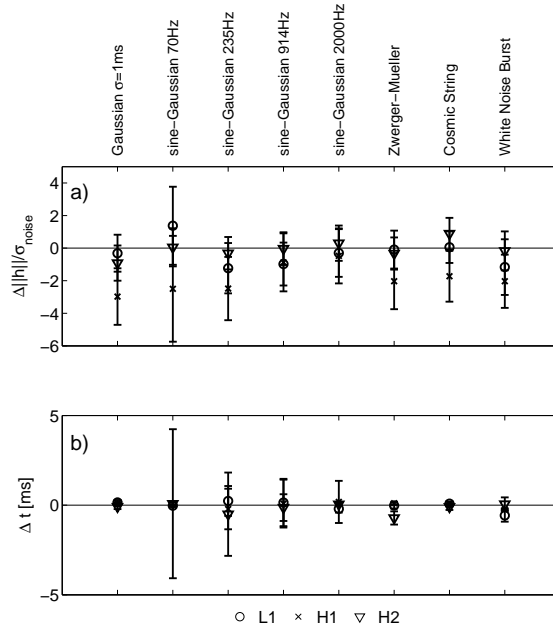


Figure 7. Measurement of a) strength and b) time of hardware injections for burst waveforms from three LIGO interferometers.

not suitable to be used for vetoing environmental events. Figure 8 shows significances of transient events around injection times, detected by the KleineWelle algorithm from two auxiliary channels, RMP and ASI, compared to injected strengths. While the events

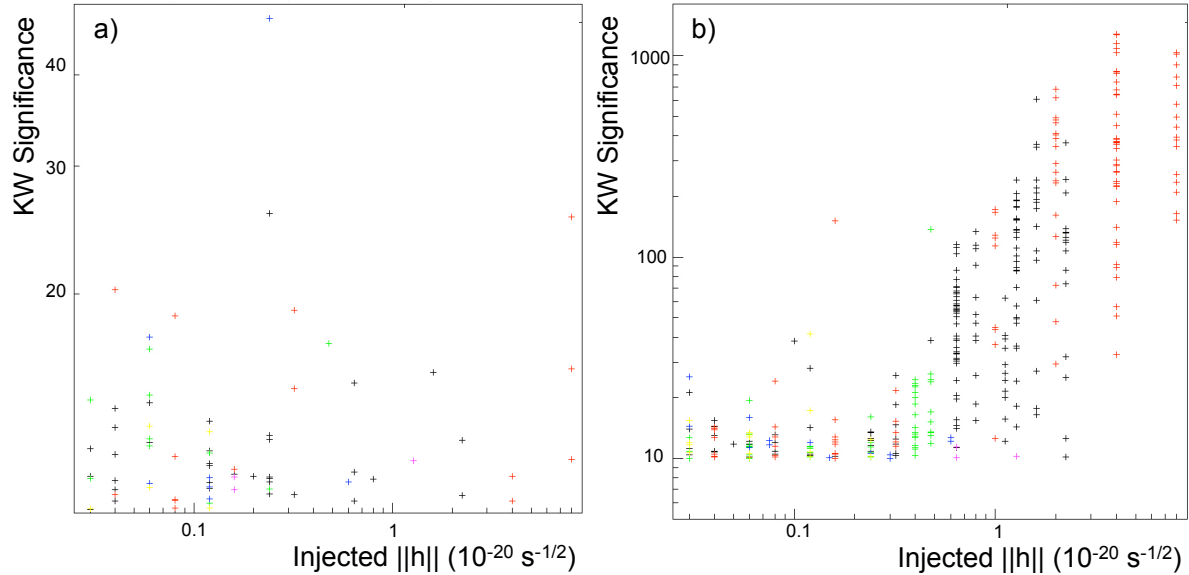


Figure 8. Examples of coupling test done with auxiliary channels, a) RMP (Recycling Mirror Pitch) and b) ASI (AntiSymmetric port In phase).

from RMP do not show a noticeable dependence on injections, those from ASI have a strong dependence on the injection, which indicates some coupling to the gravitational channel above a certain amplitude ($\sim 2 \times 10^{-21} \sqrt{s}$). The timing distribution of these

events also shows a similar result and proves that the ASI channel has some coupling to the gravitational wave channel. A more detailed report on results from this study was presented in a separate talk in this conference by Erik Katsavounidis.

7. Summary

In this report, we demonstrate how hardware injections are useful for understanding the performance of the LIGO interferometers by measuring the strength of injections and time responses of detectors. The strength and timing of the injections are measured using optimal linear filters, and compared to injected values. Hardware injections are reconstructed successfully, showing that the detector's performance is well understood. It is also shown that hardware injections are also useful to examine the coupling of auxiliary channels to the gravitational wave channel.

Acknowledgments

The authors gratefully acknowledge the support of the United States National Science Foundation for the construction and operation of the LIGO Laboratory and the Particle Physics and Astronomy Research Council of the United Kingdom, the Max-Planck-Society and the State of Niedersachsen/Germany for support of the construction and operation of the GEO600 detector. The authors also gratefully acknowledge the support of the research by these agencies and by the Australian Research Council, the Natural Sciences and Engineering Research Council of Canada, the Council of Scientific and Industrial Research of India, the Department of Science and Technology of India, the Spanish Ministerio de Educacion y Ciencia, The National Aeronautics and Space Administration, the John Simon Guggenheim Foundation, the Alexander von Humboldt Foundation, the Leverhulme Trust, the David and Lucile Packard Foundation, the Research Corporation, and the Alfred P. Sloan Foundation. This paper has been assigned LIGO document number P070036-01.

References

- [1] S. Chatterji, L. Blackburn, G. Martin and E. Katsavounidis "Multiresolution techniques for detection of gravitational-wave burst" *Class. Quantum Grav.* **21** S1809-S1818 (2004).
- [2] R. McDonough, A. Whalen, "Detection of Signals in Noise" 2nd ed.(1995) pp 201-246, *Academic Press*.
- [3] F. J. Harris "On the Use of Windows for Harmonic Analysis with the Discrete Fourier Transform." *Proceedings of the IEEE*. Vol. **66** (January 1978). pp. 66-67.
- [4] T. Zwerger and E. Müller, *Astron. Astrophys.* pp. 209-227 (1997)